

THE EFFECT OF MODAL DAMPING ON RANDOM VIBRATION METAL FATIGUE ANALYSIS

Gürzap İsmail DEMİREL¹
TÜBİTAK-SAGE
Ankara, Turkey

Prof. Dr. Altan KAYRAN²
Middle East Technical University
Ankara, Turkey

ABSTRACT

Frequency domain metal fatigue analysis is frequently used for random vibration fatigue analysis and requires frequency response (FR) of the mechanical system and the load spectrum as analysis inputs. Unit load input and the frequency response function (FRF) are used as input for the FR calculation of the system. Power spectral density (PSD) of the load is the most suitable spectrum representation of the random vibration load. Stress response profile of the mechanical system is determined via interpolating the unit load frequency response by the vibration load profile. In the frequency domain fatigue analysis, the cycle counting of the stress is done by utilizing the PSD of the stress response. Fatigue analysis of the mechanical system is then performed by using the stress-cycle (S-N) curve of the material of the mechanical system. In the vibration fatigue analysis, it is noted that the modal damping of the mechanical system is crucial because it affects the FR of the system directly. Therefore, fatigue life results are influenced by the modal damping significantly. In this study, the effect of modal damping on the vibration fatigue analysis is investigated and vibration fatigue analysis results are compared.

INTRODUCTION

Metal fatigue occurs due to repeated cyclic loads which are not high enough to cause failure within a single cycle and fatigue failure occurs when the total damage is equal to 1, according to Palmgren-Miner rule, [Fatemi and Yang, 1997]. Load cycles can be constant amplitude or variable amplitude depending on how the mechanical system is excited. Aerospace structures are subjected to mostly variable amplitude load cycles due to unexpected, unpredictable and fluctuating aeroelastic loads, [Bath and Patibandla, 2011]. The random vibration fatigue theory only covers the mechanical load based fatigue. Due to the nature of the random vibration loading, stress level is low and the deformation is primarily elastic. Therefore random vibration fatigue is in the class of high cycle fatigue. Moreover, for random vibration, the stress-life approach is more suitable rather than the strain-life approach. Strain-life approach is generally used when the stress level is high such that plastic deformation occurs, [Lee, Pan, Hathaway and Barkey, 2005].

¹MSc Student at AE, METU and Research Engineer at SAGE-TÜBİTAK, e167971@metu.edu.tr, gurzap.demirel@tubitak.gov.tr

²Prof. Dr. at Department of Aerospace Engineering, METU, akayran@metu.edu.tr

It is necessary to clarify the term vibration fatigue as the estimation of the fatigue life when the stress histories are random in nature and therefore random vibration fatigue is best specified using the statistical information about the random process. Random vibration fatigue analysis is also named as spectral fatigue analysis or frequency based fatigue technique, [Bishop, 1999].

This article deals with the random vibration fatigue analysis of notched beams by including and not including modal damping. The effect of modal damping on the vibration fatigue analysis is investigated in detail. Moreover experiments are conducted in order to verify the effect of modal damping on the vibration fatigue analysis.

THEORY

In the vibration fatigue analysis, certain definitions must be first made to aid the understanding of the methodology followed.

Power Spectral Density (PSD)

PSD is used for characterize the strength of stationary random process in the frequency domain. In order to get the PSD profiles of the random vibration loading, Fast Fourier Transform (FFT) of the random load history is taken and then PSD profile is obtained by taking the modulus of the squared FFT and divided by the $2T$, where T stands for the sample period which can also be defined as $1/f_s$ and f_s being the sampling frequency of the recorded signal, as shown in Equation 1. Figure 1 shows a typical PSD profile which has only the amplitude and frequency information. All phase and time information is discarded.

$$PSD = \frac{1}{2 * T} |FFT|^2 \quad (1)$$

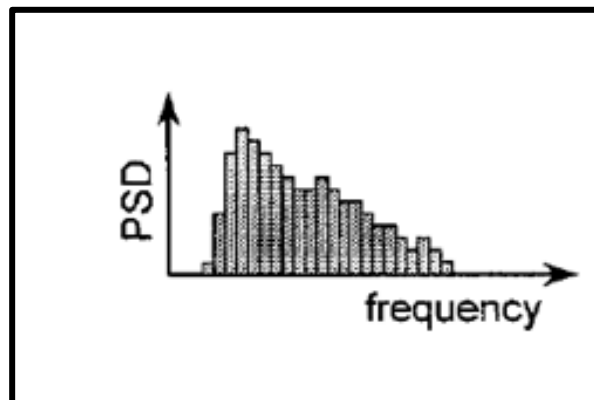


Figure 1: PSD definition, [Bishop, 1999]

The area under each spike in Figure 1 represents the mean square of the sine wave at that frequency of interest. The phase relationships between the waves cannot be determined anymore.

Some general examples of PSD profiles for different type of time histories are given in Figure 2.

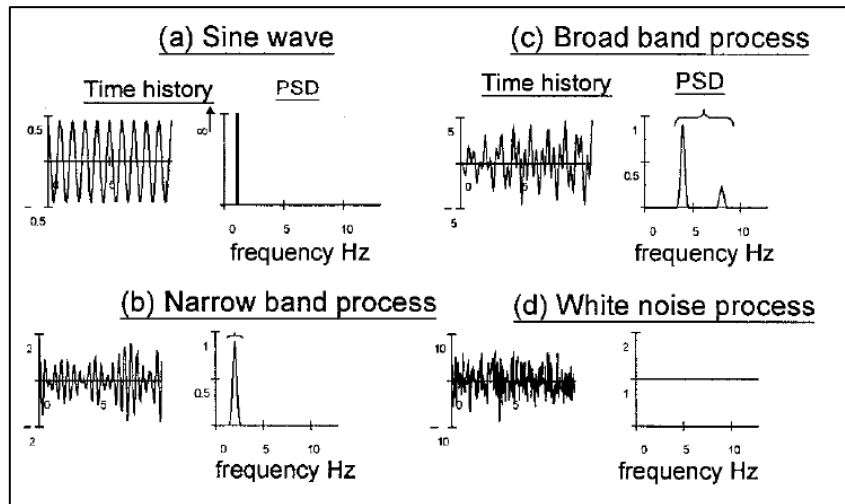


Figure 2: Different type of time histories and their PSD profiles, [Bishop, 1999]

Frequency Response

The linear structure responds to a sinusoidal force with a sinusoidal displacement at the same frequency. The transfer function is defined as the response per input at each frequency of interest. Therefore, one can predict the frequency response of the system by multiplying the load and the transfer function which is called as the frequency response function (FRF) in frequency domain calculations, as shown in Equation 2.

$$Input\ Load * FRF = Frequency\ Response \quad (2)$$

Probability Density Function (PDF)

Mathematically, the most convenient way of storing the stress range histogram is the form of PDF of stress range, [Eldoğan, 2012]. It is easy to transform from a stress range histogram to a PDF or backwards. In order to calculate the expected fatigue damage, E(D), firstly Probability Density Function (PDF) of the stress ranges, p(S), should be determined. A typical calculation of PDF is shown in Figure 3.

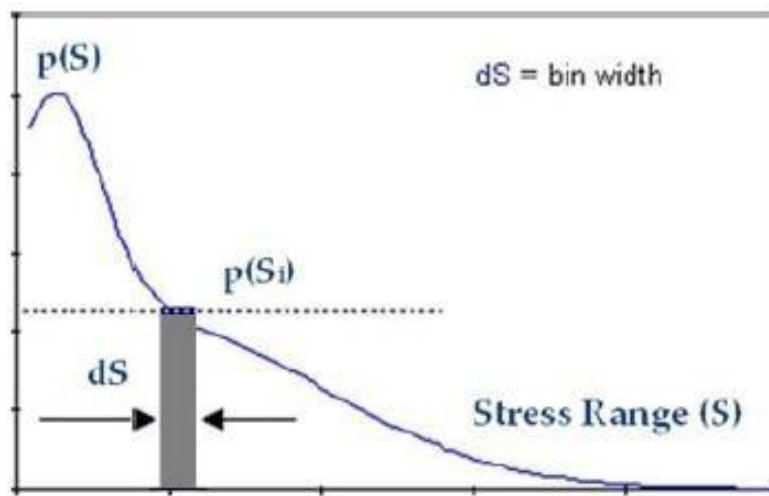


Figure 3: Calculation of PDF from stress range histogram

The bin widths, dS , and the total number of cycles in the histogram, S_t , are required in order to obtain PDF from a stress range histogram. By using the PDF, the opposite work can also be performed. Multiplication of the bin width with the value of the PDF at the stress level ($p(S_i) * dS$) gives the probability that the stress is in the range $S_i - dS/2$ and $S_i + dS/2$. Multiplying the probability of the stress range $p(S) * dS$ with the total number of cycles (S_t) in the histogram, total number of cycles, $N(S)$, for a given stress level, S , can be obtained, as shown by Equation 3.

$$N(S) = p(S) * dS * S_t \quad (3)$$

Moments of PSD Profiles

The moments of the PSD profiles are needed for the frequency domain cycle counting. The relevant spectral moments are computed from a one sided PSD [$G(f)$] in the units of Hertz using Equation 4.

$$m_n = \int_0^{\infty} f^n * G(f) * df = \sum_{k=1}^m f_k^n * G_k(f_k) * \delta f \quad (4)$$

where, δf is the frequency increment. The n^{th} moment of area of the PSD (m_n) is calculated by dividing the curve into small strips, as shown in Figure 4. The n^{th} moment of area of the strip is given by the area of the strip multiplied by the frequency raised to the power n . The n^{th} moment of area of the PSD is then found by summing the moments of all the strips. In theory, all possible moments are required to fully characterise the original process. However, in practice, m_0 , m_1 , m_2 and m_4 are sufficient to compute all of the information required for the subsequent fatigue analysis, [Bishop and Sherratt, 2000].

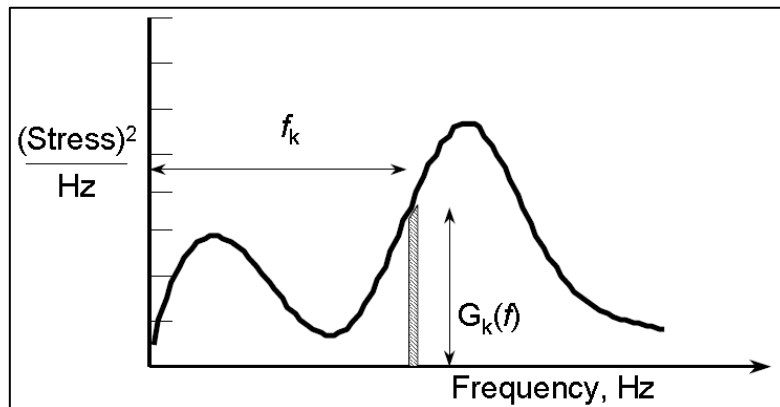


Figure 4: Calculation of the PSD moments

Frequency Domain Stress Cycle Counting

Dirlik's empirical formula for the cycle counting is the most superior in terms of accuracy, [Bishop, 1999]. Dirlik has derived an empirical closed form expression for the determination of the PDF of the cycle counting of stress ranges, which was obtained using extensive computer simulations to model the signals using the Monte Carlo technique, [Dirlik, 1985]. The Dirlik cumulative damage (D) is calculated after the cycle counting and given in Equation 5, where m and A are material properties which are the fatigue strength exponent from the material S - N curve and fatigue strength coefficient respectively.

$$D = \left(\frac{1}{2^{m \cdot A}} \right) * \int_0^{\infty} S^m * N(S) * dS \quad (5)$$

In Equation 5, Dirlik histogram formula $N(S)$ for stress cycles range is given by Equation 6,

where v_p and τ are the rate of peaks (number of expected peaks per unit time) and the exposure time respectively.

$$N(S) = v_p * \tau * p(S) \quad (6)$$

The correlation for $p(S)$ proposed by Dirlik is given in Equation 7.

$$p(S) = \frac{\frac{D_1}{Q} * e^{-\frac{Z}{Q}} + \frac{D_2 * Z}{R^2} * e^{-\frac{Z^2}{2 * R^2}} + D_3 * Z * e^{-\frac{Z^2}{2}}}{2 * \sqrt{m_0}} \quad (7)$$

where, S is the stress range and other parameters in Equation 6 and 7 are given by Equation 8.

$$D_1 = \frac{2 * (x_m - \gamma^2)}{1 + \gamma^2}, \quad D_2 = \frac{1 - \gamma - D_1 + D_1^2}{1 - R}, \quad D_3 = 1 - D_1 - D_2, \quad Q = \frac{1,25 * (\gamma - D_3 - D_2 * R)}{D_1} \quad (8)$$

$$R = \frac{\gamma - x_m - D_1^2}{1 - \gamma - D_1 + D_1^2}, \quad Z = \frac{S}{2 * \sqrt{m_0}}, \quad x_m = \frac{m_1}{m_0} * \sqrt{\frac{m_2}{m_4}}, \quad v_p = \sqrt{\frac{m_4}{m_2}}, \quad \gamma = \frac{m_2}{\sqrt{m_0 * m_4}}$$

Palmgren-Miner Rule

Palmgren-Miner rule is one of the most widely used cumulative damage models for failures caused by fatigue. The Palmgren-Miner rule states that failure occurs when linearly cumulated damage fraction (D) reaches to 1 and if there are k different stress levels and the number of cycles to failure at the i^{th} stress level (S_i) is N_i , then the damage fraction is given in Equation 9.

$$D = \sum \frac{n_i}{N_i} \quad (9)$$

where n_i is the number of applied load cycles of S_i , [Bishop and Sherratt, 2000]. The limitations of Palmgren-Miner rule are listed below;

- It assumes that all cycles of a given magnitude do the same amount of damage, whether they occur early or late in the life.
- Since Palmgren-Miner rule assumes that the cumulative damage is composed of linearly accumulated damages, the strains and stresses should stay in the elastic region.
- Palmgren-Miner rule assumes that the presence of a stress cycle of amplitude S_2 does not affect the damage caused by a stress cycle of amplitude S_1 .
- The rule governing the damage caused by a stress cycle of amplitude S_1 is the same as that governing the damage caused by a stress cycle of amplitude S_2 .

Modal Damping

Damping basically reduces the magnitude of oscillations through loss of energy. All mechanical systems possess fundamental damping property in nature. Figure 5 shows how the dynamic response of the system changes with the damping ratio (ζ). The damping characteristics of a structure are affected by geometry, stiffness, material properties, manufacturing processes and the constraint configuration, etc. If modal damping input is not supplied to the FR analysis, the FR results have unrealistically high responses. Thus, fatigue life of the mechanical system is affected significantly. This is because, when the natural frequencies of the system and input load frequencies coincide, due to the absence of damping, there are unrealistically high peaks in the

resonance region. If the real modal damping is included in the vibration fatigue analysis, the peak values of the stress response will be lower and more realistic, thereby affecting the fatigue life of the mechanical system.

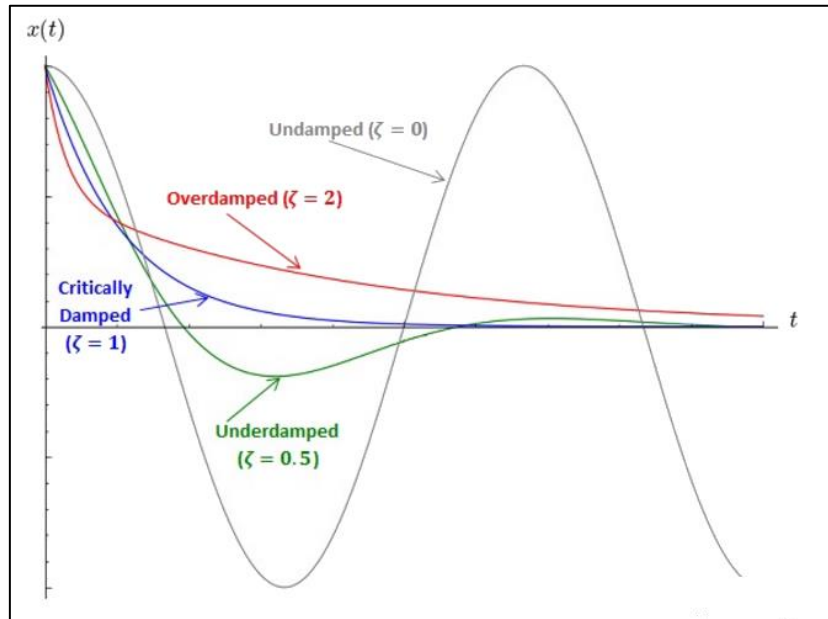


Figure 5: The effect of varying the damping ratio for mechanical system

In frequency domain, the most commonly used method of determining the damping ratio at a resonance or modal region in FRF graphs is the “3 dB Method”. This method is also called as the Half Power Method. In FRF graphs, the damping is proportional to the width of the resonance peak around the peak’s center frequency. One can determine the corresponding damping ratio by extracting the frequencies corresponding to the 3 dB below points from the peak level. Figure 6 shows an example amplitude-frequency plot which shows the 3 dB points corresponding to also the half power points. Damping ratio (ζ) is then calculated by Equation 10.

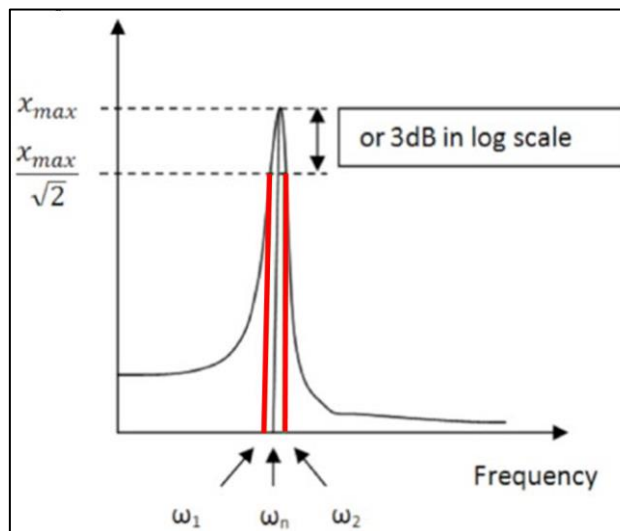


Figure 6: Half Power Method or 3 dB Method

$$\zeta = \frac{\omega_2 - \omega_1}{2 * \omega_n} \quad (10)$$

Random Vibration Fatigue Analysis Flowchart

In the present study, frequency response analysis is done by using the MSC Nastran finite element solver. MSC Patran pre-post processor is used for the finite element model (FEM) preparation. The fatigue analysis tool, nCode, is used for the random vibration fatigue analysis and post processing of the analysis results.

Basic flowchart of the random vibration fatigue analysis is given in Figure 7.

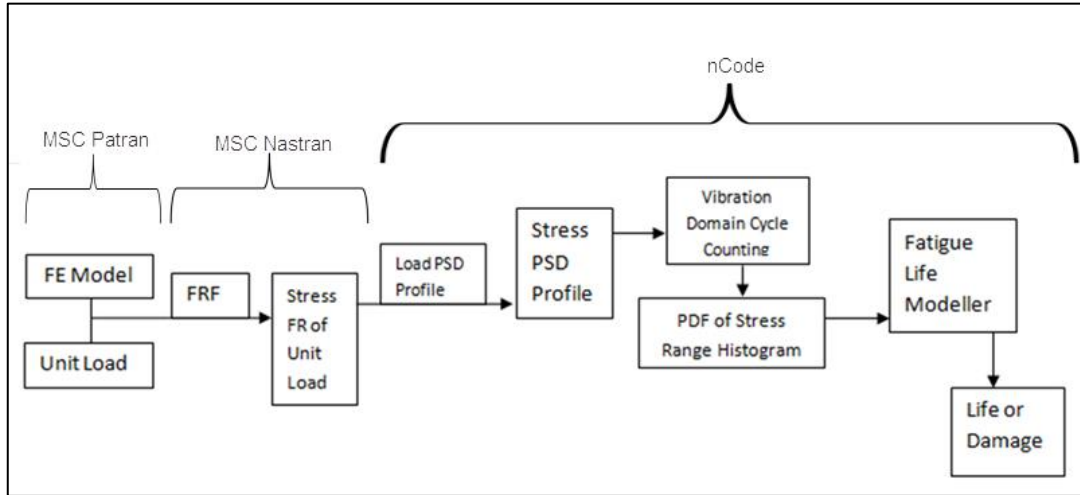


Figure 7: Basic flowchart of the random vibration fatigue analysis

In order to perform random vibration fatigue analysis for a mechanical system, firstly the FEM of the system is prepared. Then, the stress FR for the unit load input excitation of the mechanical system is determined. It should be noted that the units of the PSD and the FR of the system must be consistent. For example, if the PSD load profile has the unit as g^2/Hz , then the FR of the system should have loading unit of g or 9810 mm/s^2 , and if the PSD load profile has the unit of $(\text{mm/s}^2)^2/Hz$, then the FR of the system should have the unit input of 1 mm/s^2 .

Stress PSD profile of the mechanical system is extracted by interpolating the PSD profile of the vibration load and stress frequency response profile for unit load. The interpolation can be linear or logarithmic. The representation of PSD profile of stress histogram is given in Equation 11.

$$PSD_{stress} \left[\frac{MPa^2}{Hz} \right] = PSD_{load} \left[\frac{g^2 \text{ or } \left(\frac{mm}{s^2} \right)^2}{Hz} \right] * \left(\text{Stress FR profile for unit load} \left[\frac{MPa}{g \text{ or } mm/s^2} \right] \right)^2 \quad (11)$$

The vibration domain cycle counting is performed to get the PDF of the stress range histogram which allows the calculation of the total number of cycles for the stress levels via Equation 6. At the last step, in the fatigue life modeler, Equation 5 is employed to calculate the fatigue damage induced due to the vibration load profile applied to the mechanical system.

ANALYSIS OF NOTCHED BEAMS

In order to investigate the effect of modal damping on the vibration fatigue analysis results, modal damping of aluminum beams are measured to have realistic modal damping values in fatigue analysis. For this purpose, notched aluminum beams made of Al-6061-T6 are

manufactured. Table 1 gives the material properties of the Al-6061-T6 material.

Table 1: Mechanical properties of Al-6061-T6

Elastic Modulus	Poisson's Ratio	Density	Tensile Yield Strength	Ultimate Tensile Strength
68.3 GPa	0.33	2710 kg/m ³	276 MPa	310 MPa

Figure 8 shows the geometry of the notched beam.

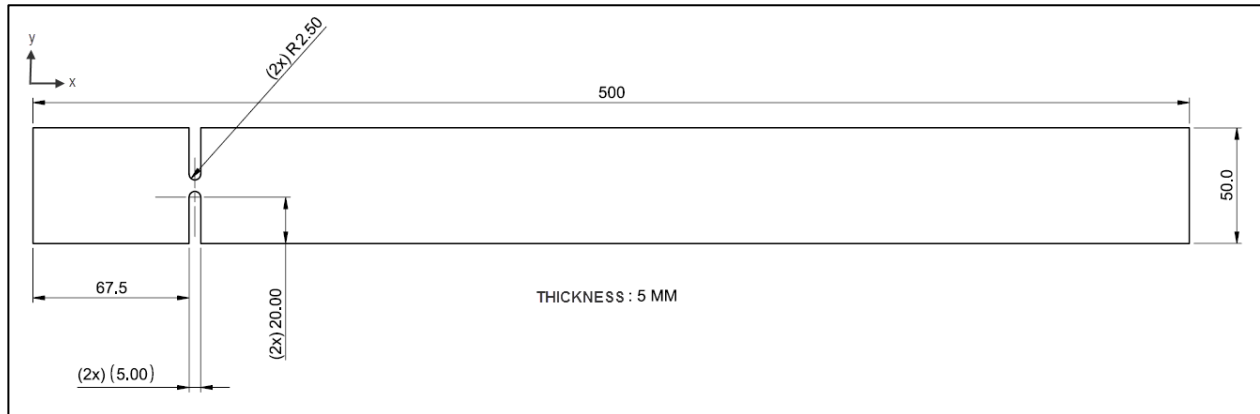


Figure 8: Geometry of aluminum notched beams, [mm]

The modal damping ratios of the mechanical systems vary mainly depending on the constraint mechanisms and excitation configurations of the mechanical system and also on other parameters. The excitation of beams is configured to disturb only out-of-plane modes which are in the z direction shown in Figure 8.

Preliminary Modal Analysis

In order to decide the test and analysis frequency interval of interest, to place the test devices properly and to prevent misreading the test data, the preliminary modal analyses are performed by MSC Patran pre-post processor and MSC Nastran finite element solver. Before performing the modal analyses, mesh refinement work is carried out. The finite element model (FEM) of the beams includes QUAD8 type two dimensional quadratic shell elements. Displacement boundary conditions are applied for a distance of 50 mm from the left-side of the beams according to Figure 8. The mesh refinement study is carried out with the inertial load as 9810 mm/s^2 which is gravitational acceleration. After the mesh refinement analyses, it is decided to use a global edge length of 2.5 mm away from the notch and an element size of 0.5 mm mesh seed is applied to the notched region of the beam. Table 2 gives the result of the mesh refinement study.

Table 2: Mesh refinement results

Global Edge Length (mm)	Notched Region Mesh Seed (mm)	Stress (MPa)
10	10	43,2
10	5	36,6
5	1	43
5	0,5	43,1
2,5	0,5	43,1

Finite element model of the beam is given in Figure 9 and notched side in Figure 10. Finite element model includes 12586 nodes and 4015 QUAD8 elements.

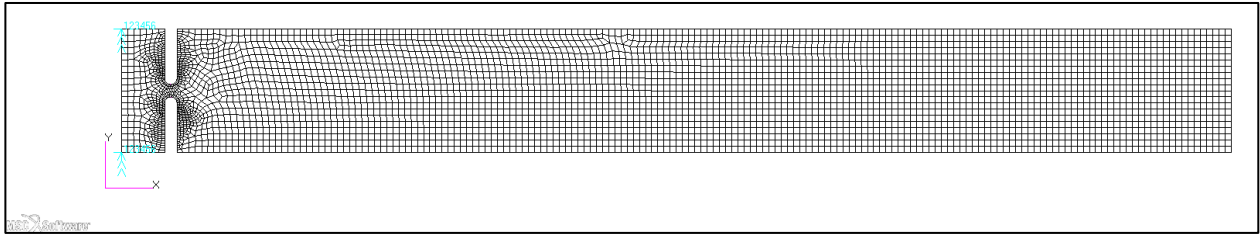


Figure 9: Finite element model of the notched beam

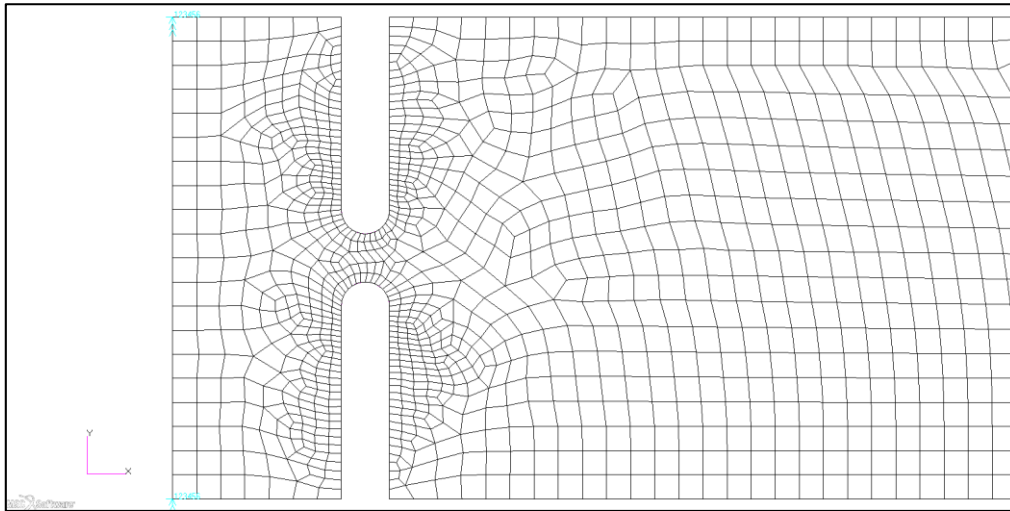


Figure 10: The mesh of the notched region

In order to decide how many modes to include in the vibration fatigue analysis, modal effective mass fraction of the beam is calculated. Modal effective mass is a measure to classify the importance of a mode shape when a structure is excited by base acceleration. A high effective mass will lead to a high reaction force at the base, while mode shapes with low modal effective mass will give low reaction forces at the base. To determine the modal effective mass, while performing the vibration analysis MSC Nastran, “MEFFMASS(ALL)=YES” command inserted to the input file of the MSC Nastran. Modal effective mass result of the analysis for the x (T1), y (T2) and z (T3) vibration response directions is given in Table 3. If the summation of the modal effective mass in any selected response direction is between 80% and 90%, it is considered to be sufficient to capture the dominant dynamic response of the structure according to current engineering experiences.

Table 3: Modal effective mass result of the modal analysis, [Hz]

MODE NO.	FREQUENCY	MODAL EFFECTIVE MASS FRACTION (FOR TRANSLATIONAL DEGREES OF FREEDOM)							
		T1		T2		T3			
		FRACTION	SUM	FRACTION	SUM	FRACTION	SUM		
1	1.510841E+01	7.667216E-30	7.667216E-30	6.349992E-22	6.349992E-22	6.677976E-01	6.677976E-01		
2	2.879853E+01	3.787574E-17	3.787574E-17	7.204307E-01	7.204307E-01	5.948523E-22	6.677976E-01		
3	1.098479E+02	1.330372E-30	3.787574E-17	6.719061E-26	7.204307E-01	1.712675E-01	8.390651E-01		
4	2.599823E+02	6.557577E-31	3.787574E-17	2.501120E-27	7.204307E-01	4.121037E-10	8.390651E-01		
5	3.260713E+02	3.499450E-31	3.787574E-17	3.788799E-28	7.204307E-01	5.178088E-02	8.908460E-01		
6	6.588857E+02	9.569457E-29	3.787574E-17	7.250012E-27	7.204307E-01	2.544945E-02	9.162954E-01		
7	8.420721E+02	9.000964E-28	3.787574E-17	6.345860E-26	7.204307E-01	2.672723E-10	9.162954E-01		
8	9.210046E+02	8.727772E-12	8.727810E-12	1.391909E-01	8.596215E-01	3.167701E-28	9.162954E-01		
9	1.105891E+03	1.674558E-23	8.727810E-12	3.158570E-23	8.596215E-01	1.573241E-02	9.320278E-01		
10	1.504892E+03	2.279974E-21	8.727810E-12	5.621480E-22	8.596215E-01	1.253555E-09	9.320278E-01		

Table 4 gives the first four modes of the out-of-plane (z direction/T3) vibration modes. According to Table 4, first four out-of-plane modes constitute 91.63 % of the modal effective mass.

Table 4: Out-of-plane translational modes of the beam

Mode	Hz	Modal Effective Mass Fraction (%)	Cumulative Modal Effective Mass (%)
1	15.1	66.78	66.78
2	109.8	17.13	83.91
3	326.1	5.18	89.09
4	658.9	2.55	91.64

The 4 out-of-plane translational modes of the beam are selected and the frequency interval of the analysis/experiment works is decided to be from 1 Hz to 700 Hz.

Modal Testing of Beams

In order to extract the modal damping ratios of the notched aluminum beams, modal testing is carried out. In the vibration testing, 4 accelerometers, 1 load cell, 1 modal exciter and 1 clamp are used. The sensors and test devices are positioned according to the information from the preliminary modal analysis to prevent the misreading of the test data or false positioning of the accelerometer on the nodal points on the modes. For example, mode 4 has 3 nodal points away from the zero displacement constraint. The displacement constraint is adjusted according to clamp and exciter positions. The load cell is placed at the tip of exciter and on the opposite side of the Accelerometer 1. The schematic of the final positioning of the load cell and the accelerometers on the beam is given in Figure 11.

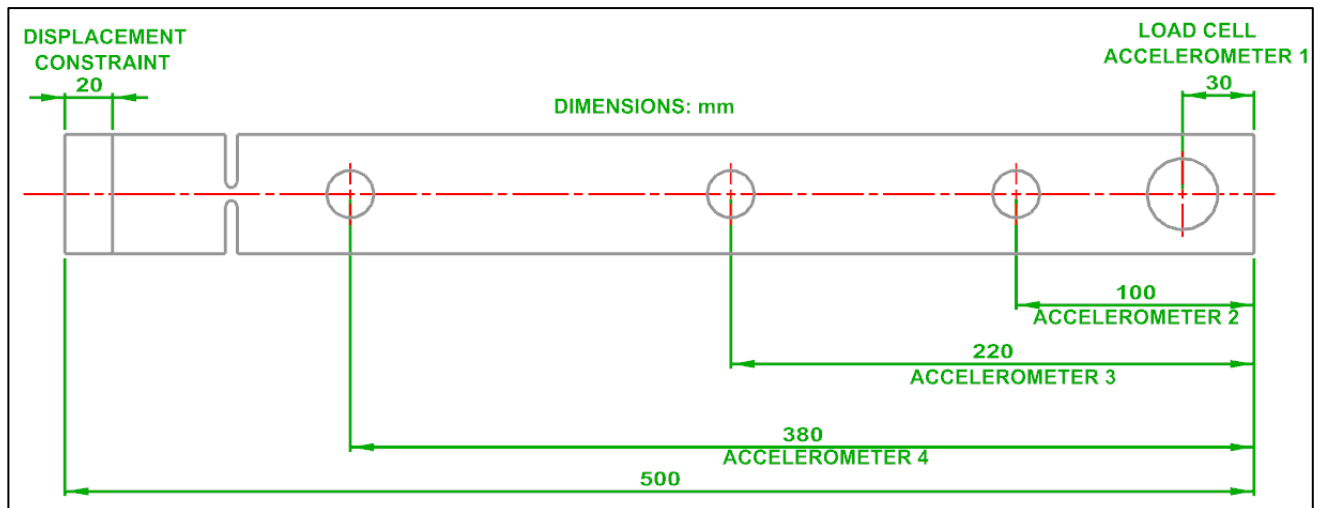


Figure 11: Positioning of the accelerometers on the beam

While performing the modal test, LMS12A software is used. The test setup is given in Figure 12.

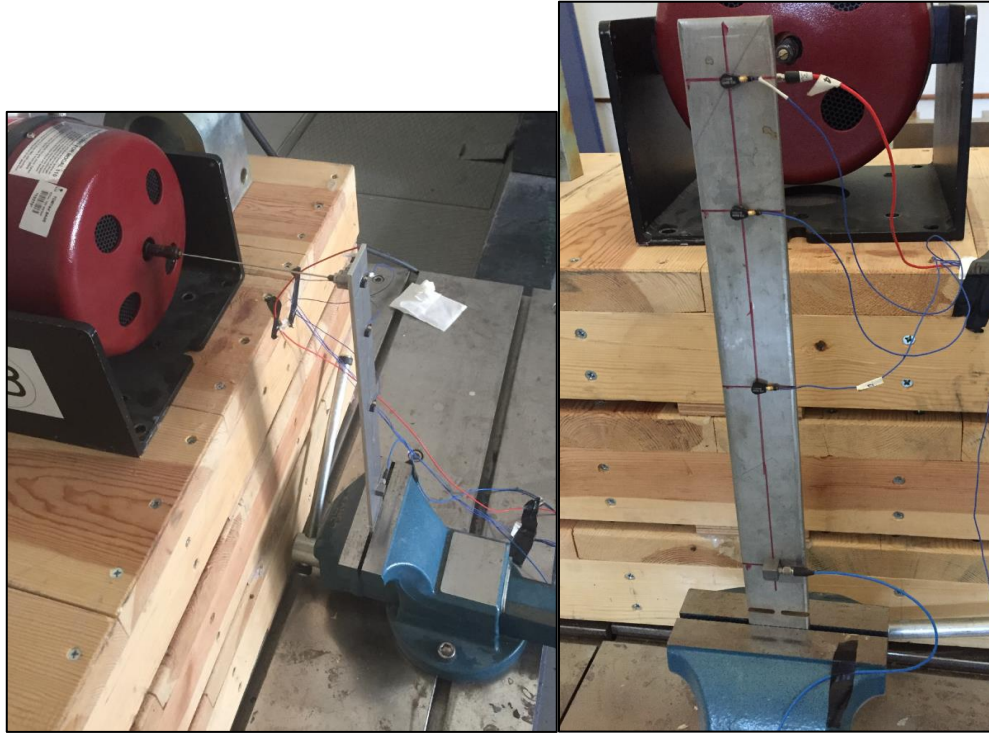


Figure 12: Vibration test setup for the notched beam

In order to extract the damping ratio of the modes appropriately, the sine sweep tests with 0.001 Hz frequency resolution are conducted. The results of the sine sweep signal tests are given in Table 5.

Table 5: Frequencies and modal damping ratios of the first four out-of-plane translational modes of the notched beam

Test Result	Mode number	Hz	Damping ratio (%)
Mode 1 : 13.570 Hz, 0.29 %	1	13.57	0.29
Mode 2 : 101.419 Hz, 0.09 %	2	101.419	0.09
Mode 3 : 295.783 Hz, 0.61 %	3	295.783	0.61
Mode 4 : 597.826 Hz, 0.07 %	4	597.826	0.07

In order to compare the natural frequency results of the test and natural frequency results of the analysis, the modal analysis is performed with updated test boundary conditions.

Modal Analysis with Test Boundary Conditions

While performing the modal test of the beam, the real displacement constraint was 20 mm due to the clamp, test specimen, modal shaker configuration. The modal analysis with the test boundary conditions and the preliminary modal analysis differ only in the length of the displacement constraint. Moreover, the mass of accelerometers are assumed as negligible for the test because the beam is 350 grams approximately and Accelerometer 1, 2, 3 are 0.8 grams each. In addition, Accelerometer 4 is 7.5 grams but it is very close to displacement constraint. The global edge length of the FEM and material properties are as same as in the preliminary modal analysis. The FEM of the beam is given in Figure 13 and the FEM includes 14047 nodes and 4450 QUAD8 elements.

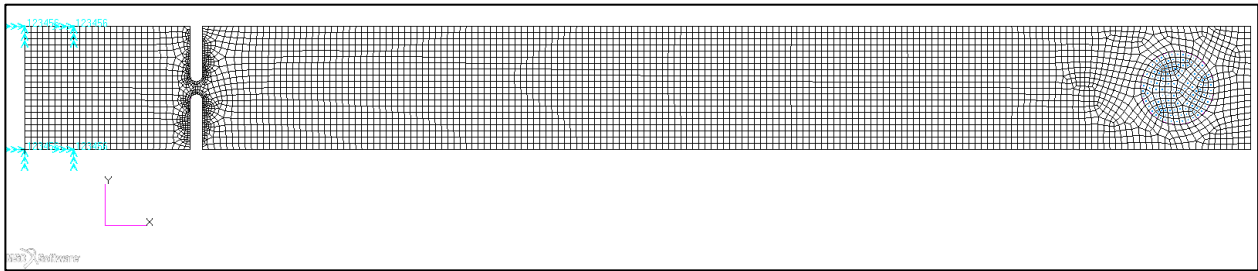


Figure 13: Finite element model of the notched beam with test boundary conditions

The select first four out-of-plane translational modes, which are in z direction and correspond to T3 in MSC Nastran, are given in Table 6.

Table 6: Out-of-plane translational modes obtained by the modal analysis for the notched beam with the test boundary conditions

Mode	Hz
1	13.984
2	103.98
3	306.13
4	604.33

The 1st mode shape of the beam is given in Figure 14.

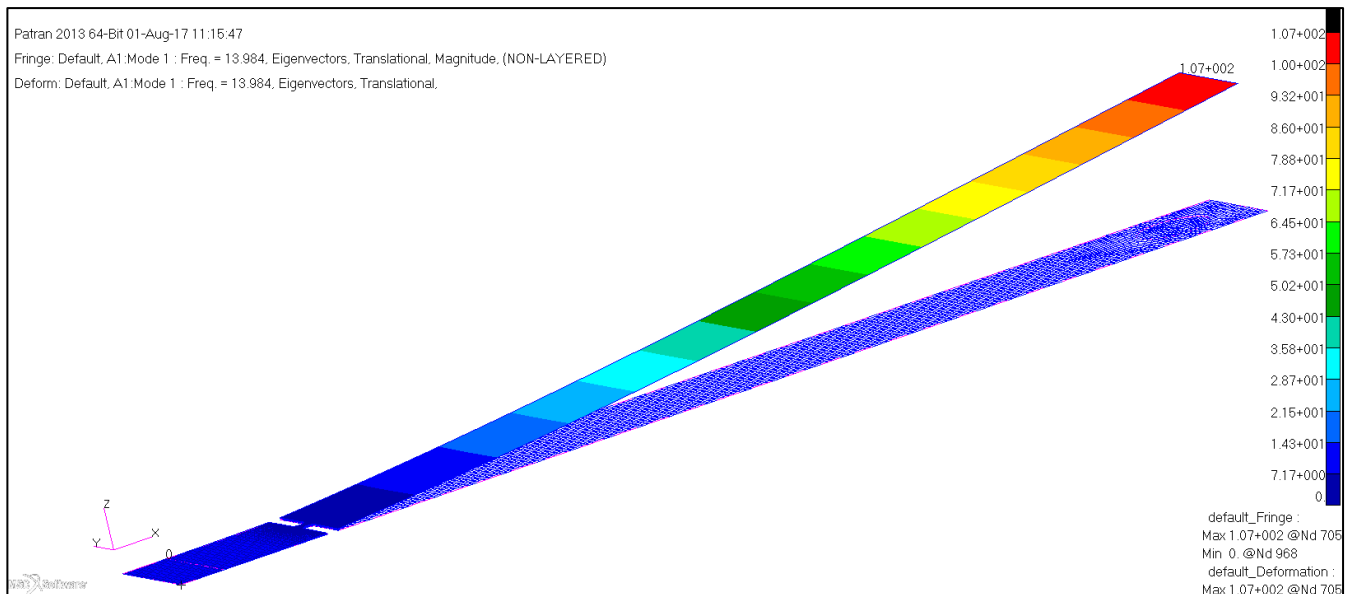


Figure 14: 1st mode shape of the beam

The 2nd mode shape of the beam is given in Figure 15.

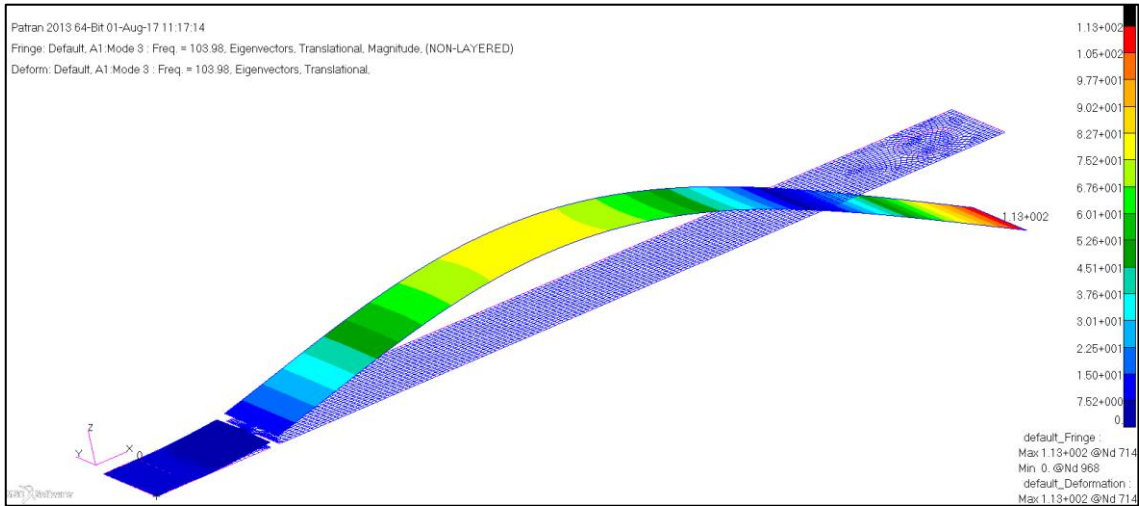


Figure 15: 2nd mode shape of the beam

The 3rd mode shape of the beam is given in Figure 16.

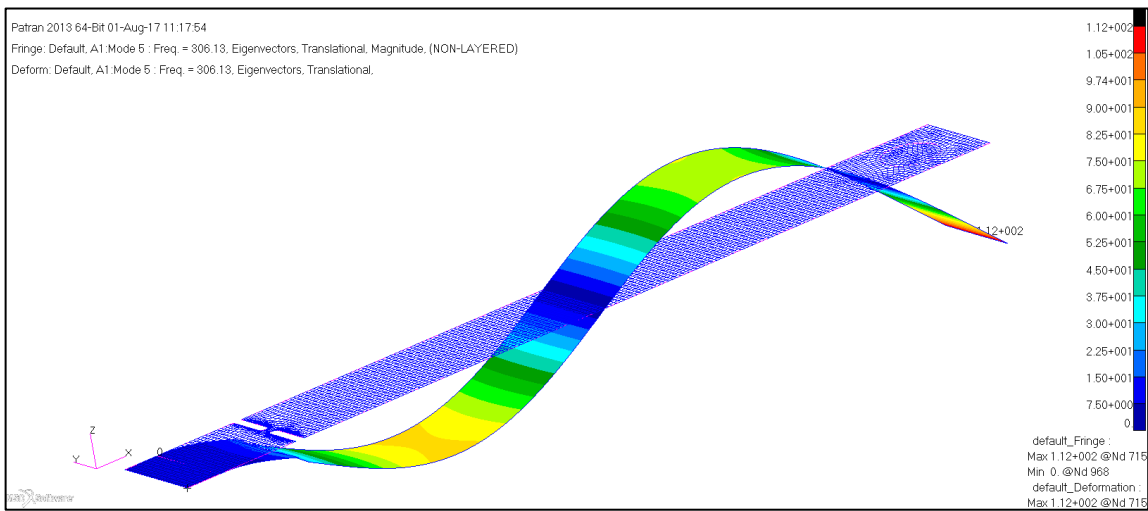


Figure 16: 3rd mode shape of the beam

The 4th mode shape of the beam is given in Figure 17.

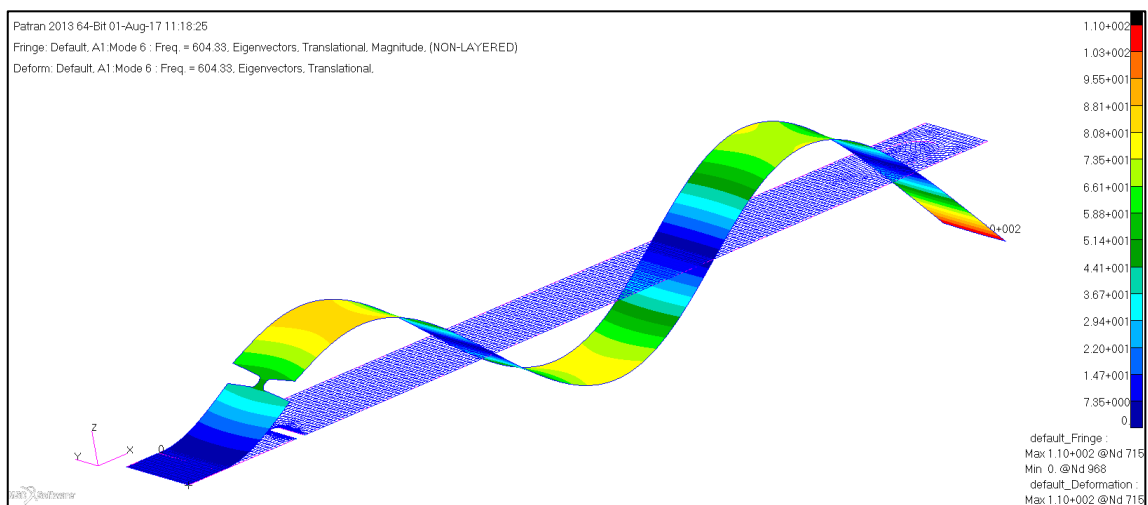


Figure 17: 4th mode shape of the beam

The comparison table of analysis and test results is given in Table 7.

Table 7: The comparison table of modal analysis and test results

Mode	Analysis (Hz)	Test (Hz)	Deviation (%)
1	13.984	13.57	2.96
2	103.98	101.419	2.46
3	306.13	295.783	3.38
4	604.33	597.826	1.08

The test and analysis results of the beam do not make a perfect agreement but they are in acceptable interval for this specific study because this study interests mainly in modal damping ratio effect on the vibration fatigue analyses. The disagreements may occur from test setup equipment, manufacturing processes, misalignment of test items etc. Especially, the test setup for this specific study has not perfectly proper constraint mechanisms as shown in Figure 12. The clamp has its own modes which they may affect the test specimen's modes. Moreover the clamp is not perfectly stiff in order to use as constraint mechanisms. However, because of the lack of the FEM model of the clamp, it cannot be included to analysis and the test specimen or the notched beam is assumed to be perfect as constraint mechanism.

Frequency Response Analysis

While performing the frequency response analysis with MSC Patran and MSC Nastran, the beam is subjected to the base acceleration load of amplitude 1 mm/s^2 in z-direction through the left 20 mm side of the notched beam according to Figure 8.

The prepared FEM and the applied load for the frequency response analysis is given in Figure 18. The frequency interval of analysis is set as 1 Hz to 700 Hz.

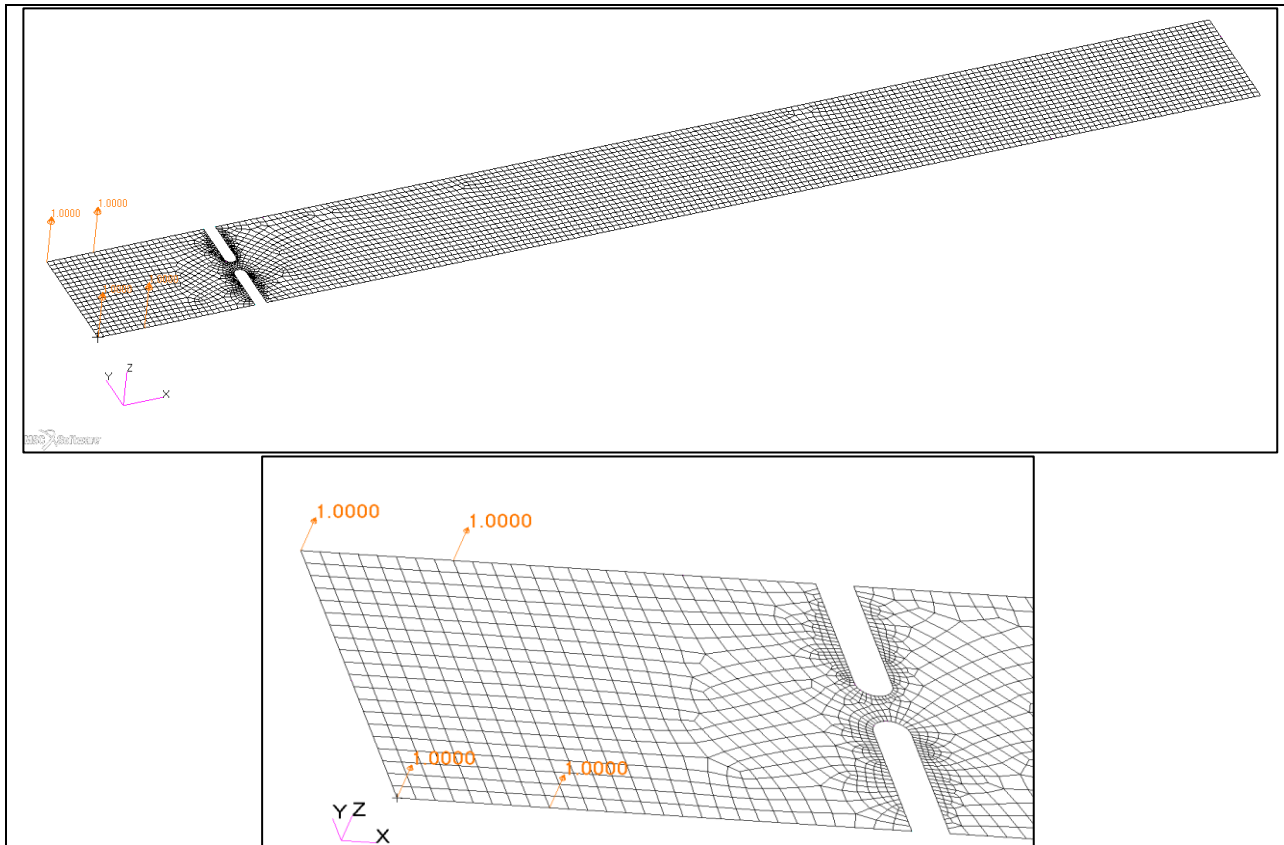


Figure 18: The FEM of the frequency response analysis

Firstly, the frequency response analysis is carried out without including the modal damping in the analysis model (undamped case). The stress frequency response of the notched beam is extracted from the node which is at the notched region, as shown in Figure 19.

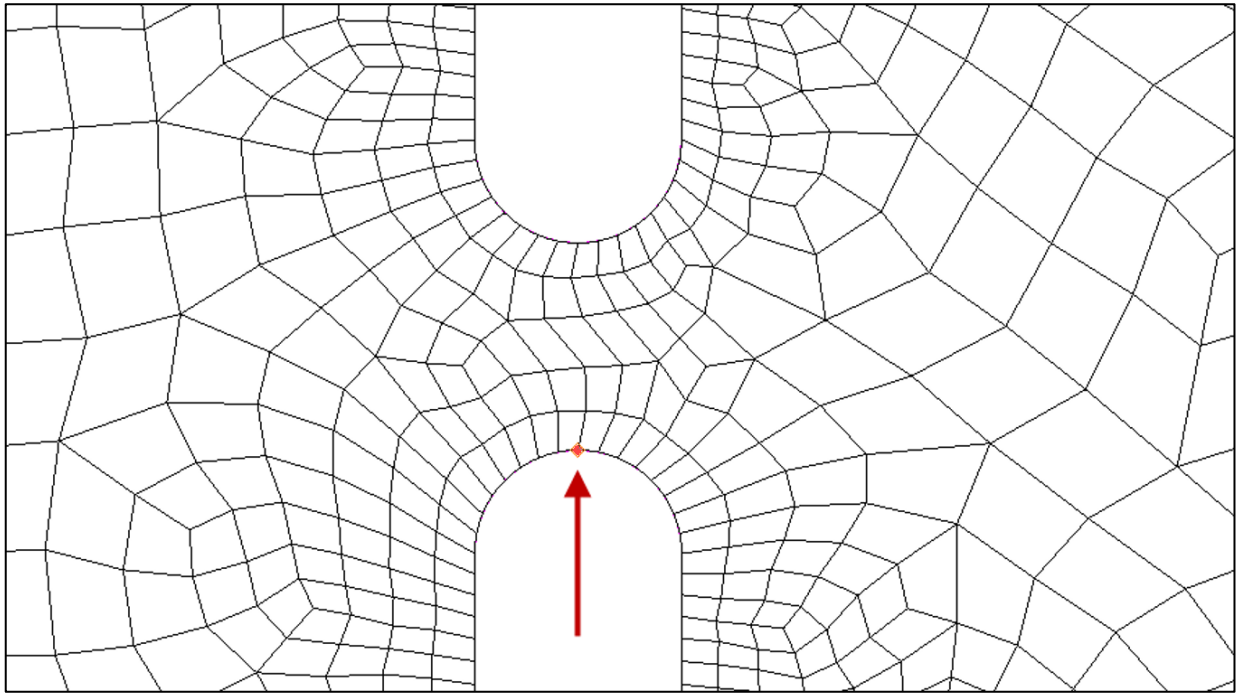


Figure 19: Finite element node where the stress frequency response is calculated

The von Mises stress frequency response of the node in the undamped case analysis model is given in Figure 20.

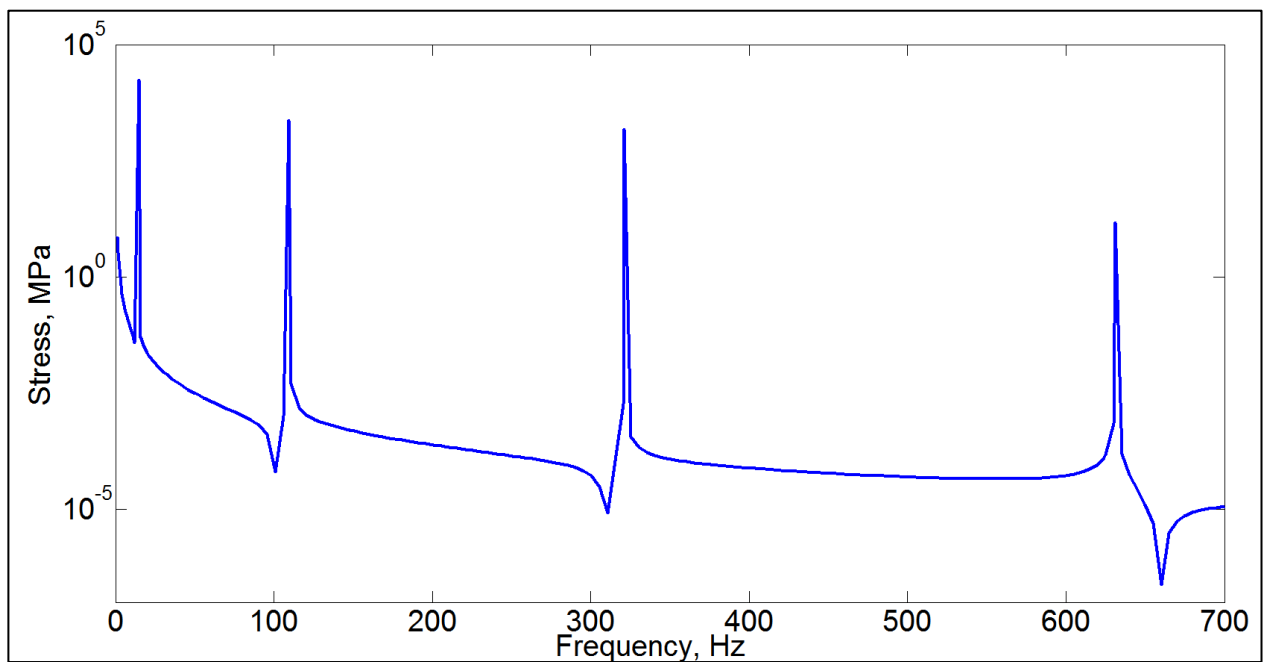


Figure 20: The von Mises stress frequency response of the node at notched region, undamped case, [MPa]

Secondly, analysis is carried out by including the modal damping to compare the vibration fatigue analysis results.

In the literature, there are lots of information about the damping ratio values such as 2% for aluminum and 3% for steel type materials. However, this approach is not perfectly accurate because each mode of the mechanical system has their own characteristic properties which depend on parameters such as constraint mechanisms, geometry of the structure, heat treatment of the material etc. If the modal damping ratio of the mechanical system is not available or there is no possibility to test the structure, then constant damping ratios available in the literature can be used in order to get preliminary results.

The modal damping ratios of the notched beam, given in Table 5, are entered into the analysis by MSC Patran “Modal Damping” table and other analysis options and parameters are taken as same as without the damping case. While inserting the modal damping ratios into the analysis, the values should multiplied by 2 because of the Structural Damping (G) is selected, [MSC. Software, 2013]. The relationship between the Damping Ratio (ζ) and Structural Damping (G) is given in Equation 12 and the inserted Structural Damping (G) values is given in Table 8.

$$G = 2 * \zeta \quad (12)$$

Table 8: Structural Damping (G) table of the notched beam

Frequency (Hz)	Value
13.984	0.0058
103.98	0.0018
306.13	0.0122
604.33	0.0014

The von Mises stress response of the node with modal damping ratios is given in Figure 21.

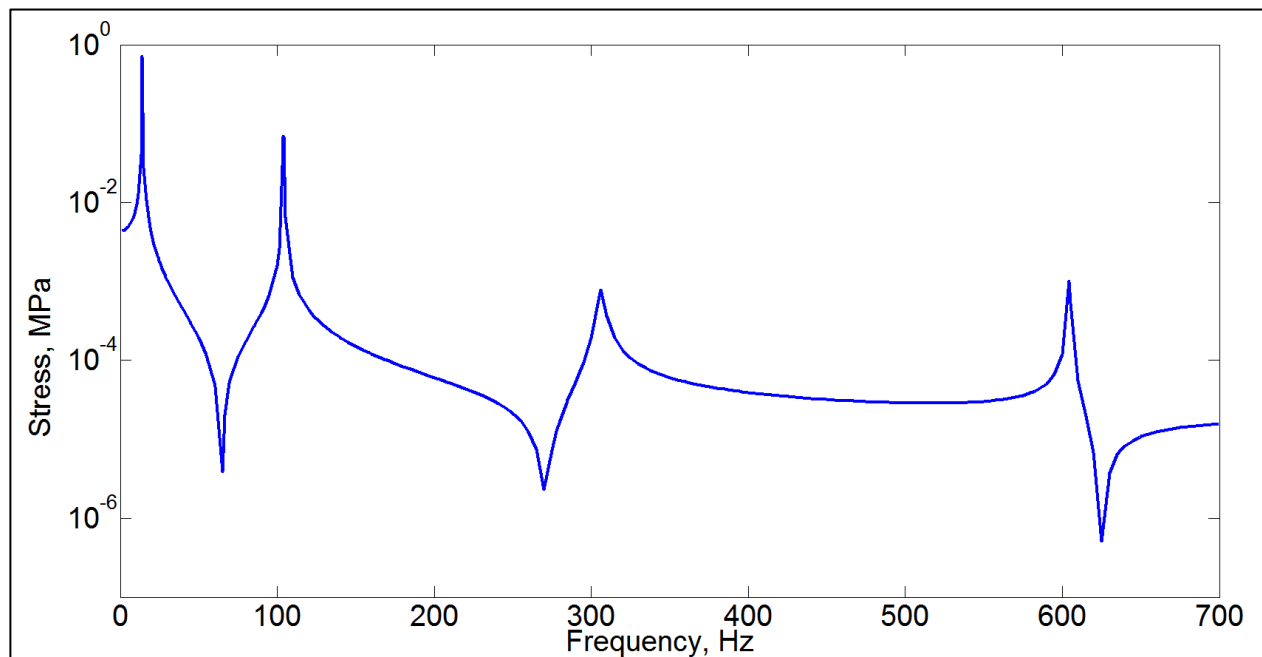


Figure 21: The von Mises stress frequency response of the node at the notched region, with modal damping case, [MPa]

Vibration Fatigue Analysis

In order to conduct the vibration fatigue analysis, the nCode software is used. This software has the Vibration CAE Fatigue Engine which is specifically used in vibration fatigue analysis. In the present study, for the vibration fatigue analysis, the applied PSD of the vibration load is taken as white noise from 1 Hz to 700 Hz with 10000 $(\text{mm/s}^2)^2/\text{Hz}$ amplitude. Moreover the Dirlik option is selected as the “VibrationLoad_PSDCycleCountMethod” and “VibrationLoad_ExposureDuration” is set to 1 second.

The PSD of the white noise vibration load profile used in the vibration fatigue analysis is given in Figure 22.

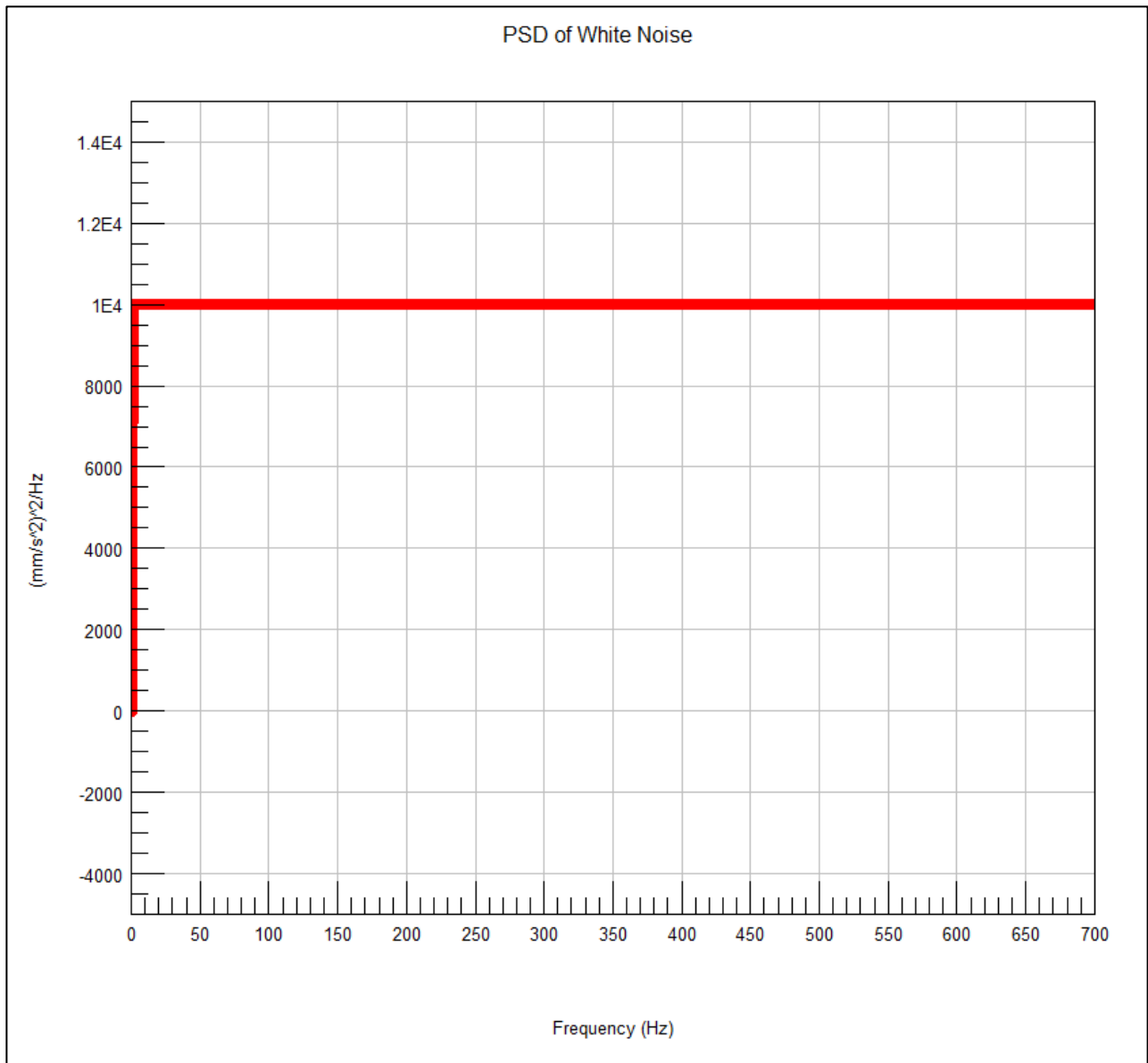


Figure 22: The PSD of the white noise vibration load profile, $[(\text{mm/s}^2)^2/\text{Hz}]$

In nCode, the “VibrationAnalysis” is the engine which makes the fatigue damage and life calculations. The analysis setup used in this study is given in Figure 23.

Name	Value	Description
General		
LoggingLevel	Info	The amount of detail to output to the message window during the run
ResultsUpdateInterval	10	Time interval between processing result output
AnalysisGroup		
AnalysisGroup_GroupNames	*	Groups to process
AnalysisGroup_MaterialAssignmentGroup	SelectionGroup	Sets the grouping type to be used for material mapping
AnalysisGroup_SelectionGroupType	FEInput	Sets the grouping type to be used for extracting results
AnalysisGroup_ShellLayer	Top	Shell layer to use
AnalysisGroup_SolutionLocation	AveragedNodeOnElement	Solution location
AnalysisGroup_StressUnits	MPa	The units to use for stress values
Compressed results (for display)		
Compressed results (for display)_ChannelPerEvent	False	Whether to create a channel for each duty cycle event
Job		
Job_NumAnalysisThreads		The number of simultaneous analysis threads to use for this job
SNEngine		
SNEngine_CertaintyOfSurvival	90	Required confidence level on damage results
SNEngine_CombinationMethod	AbsMaxPrincipal	The method used to combine component stresses/strains
SNEngine_MeanStressCorrection	None	The method used to correct the damage calculation for mean stress
SNEngine_OutputEventResults	False	Whether to output results per event or not for duty cycle processing
VibrationLoad		
VibrationLoad_ExposureDuration	1	Exposure duration in seconds
VibrationLoad_FrequencySelectionMethod	LoadingAndFRFFrequencies	Method used for selecting frequency points
VibrationLoad_InterpolationMethod	LinLin	Method to use when interpolating the loading spectra
VibrationLoad>LoadingMethod	PSD	Vibration loading method
VibrationLoad_PSDCycleCountMethod	Dirlik	PSD cycle count method
VibrationLoad_SweepRate	1	Sweep rate applied in terms of the sweep type
VibrationLoad_SweepType	LinearHzPerSec	Sweep type using sweep rate provided

Figure 23: “VibrationAnalysis” engine of nCode for setting up the vibration fatigue analysis

RESULTS

The life results of the random vibration fatigue analyses, which are the time for the crack initiation, of undamped and with modal damping cases are given in Figure 24 and Figure 25, respectively. Figures 24 and 25 give the life in terms of the repeats of the exposure duration of the vibration load. The exposure duration of the vibration load is set to 1 second in this study. As seen in Figure 24, the minimum number of repeats is approximately 0.003 at the notched region which means that the fatigue life of the notched beam is 0.003 s because of the load exposure duration time is 1 second. However, when modal damping is included in the vibration fatigue analysis, minimum number of repeat has increased to approximately 10360 repeats which means that the life in terms of seconds is 10360 seconds or approximately 3 hours, as seen in Figure 25.

It is seen that including the modal damping significantly increases the fatigue life of the notched beam. Considering that the load exposure time is 1 s, when modal damping is included, the notched beam virtually has infinite fatigue life within the comparison of undamped case. However, it should be recalled that present fatigue life results are valid for the amplitude of 10000 (mm/s²)/Hz for the PSD of the white noise and depending on the amplitude of the PSD of the vibration load, fatigue life results may change radically.

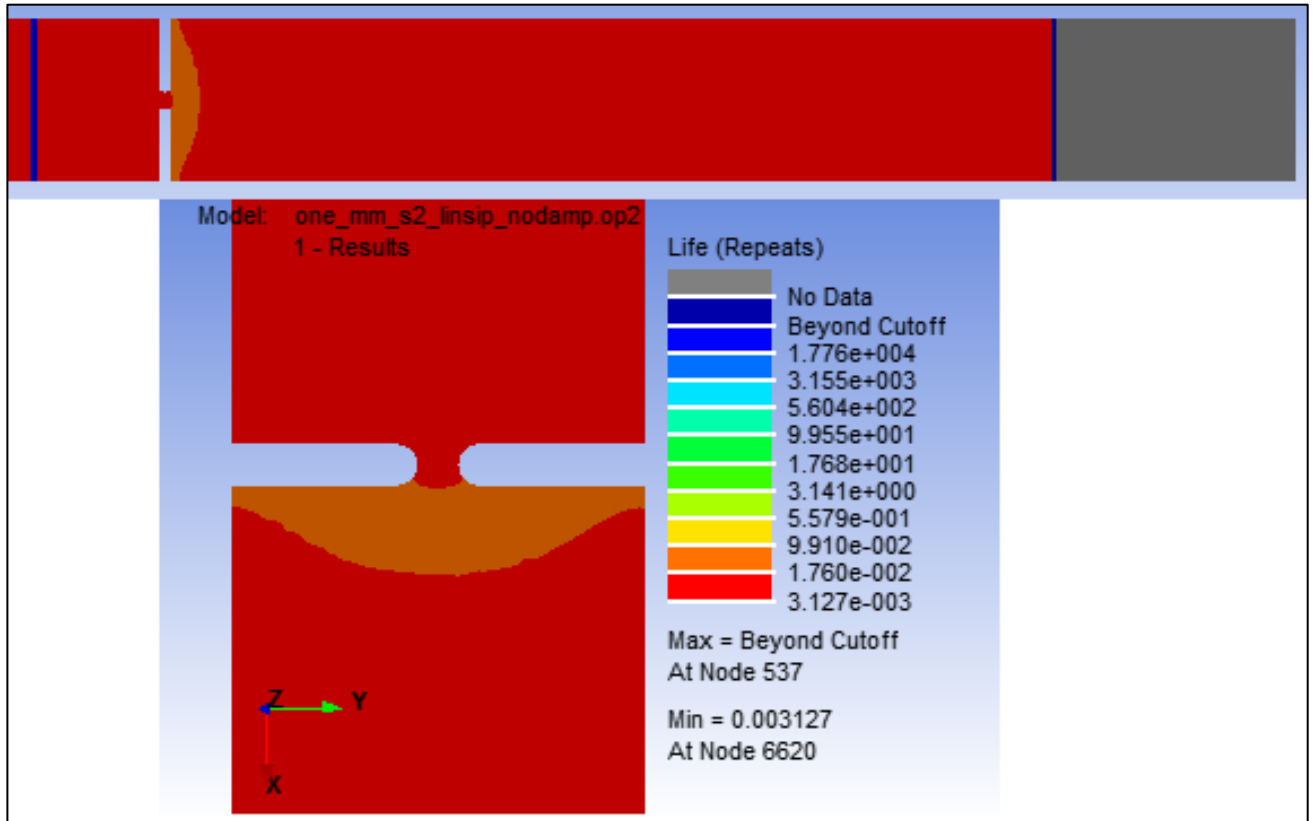


Figure 24: Random vibration fatigue analysis result, undamped case

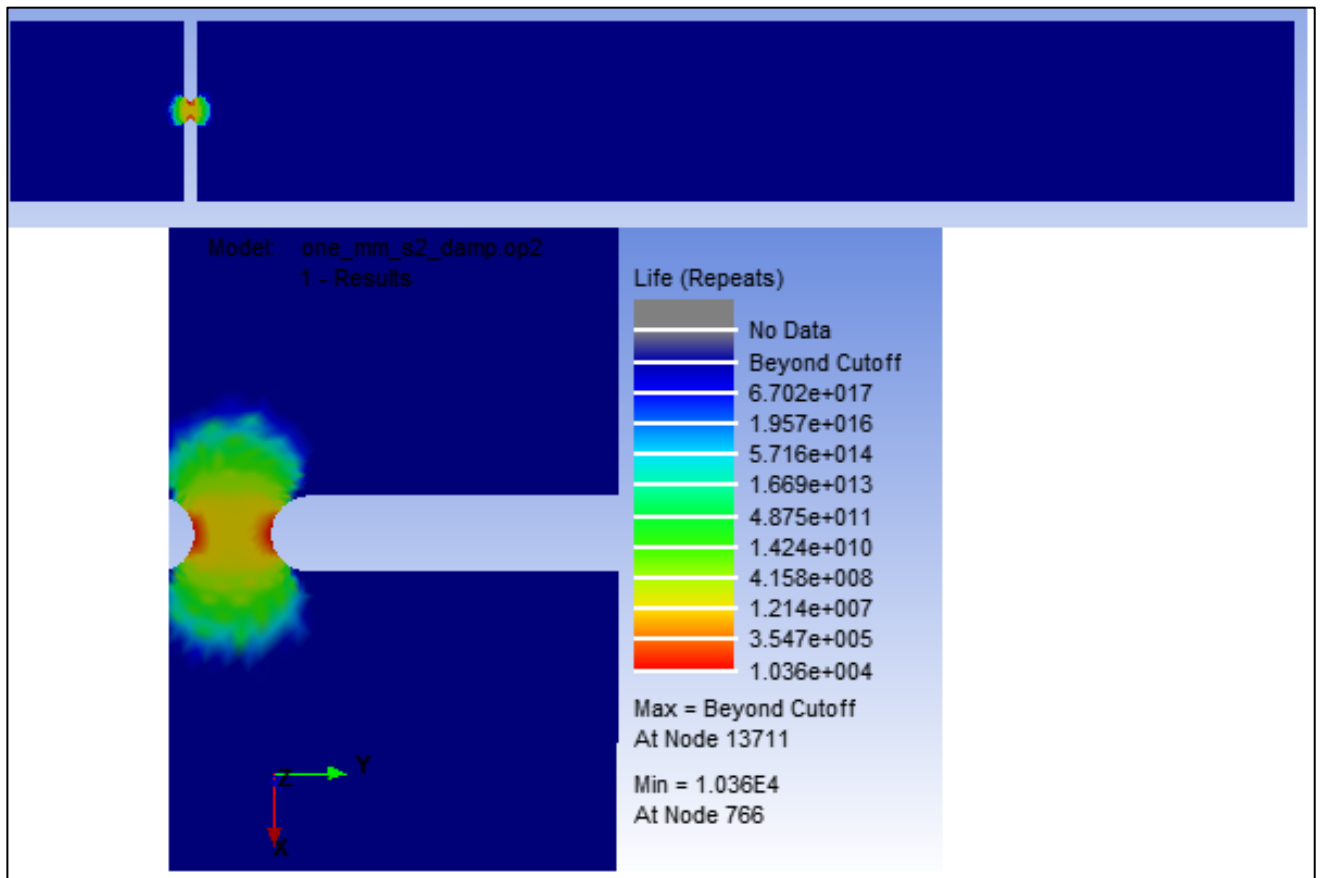


Figure 25: Random vibration fatigue analysis result, with modal damping case

According to Figure 24, almost the whole averaged nodes on elements of notched beam go under the failure within the 0.003 seconds. In this study, the failure term corresponds to the crack initiation. The reason is that the stress frequency response profile to unit load of the undamped case has unrealistically high stresses in the resonance regions or the natural frequencies of the beam. Figure 20 has the stresses such that they are above the elastic stress-strain regions and also above the ultimate strength of the material of the beam. In fact, the beam goes under the static failure according to the stress frequency response profile to unit load of the beam, Figure 20. However, the with modal damping case has the stresses too low from the yield stress of the material of the beam, Figure 21. This realistic stress response profile gives the more realistic and reliable fatigue life results.

The stress responses to unit load of the beam at the first out-of-plane translational mode, 13.984 Hz, of the undamped and with modal damping case are given in Figure 26 and Figure 27 respectively. In order to provide visual clarity, the upper threshold for the stress result of the undamped case is set to ultimate tensile strength of the material which is 310 MPa for 6061-T6 type aluminum, Table 1.

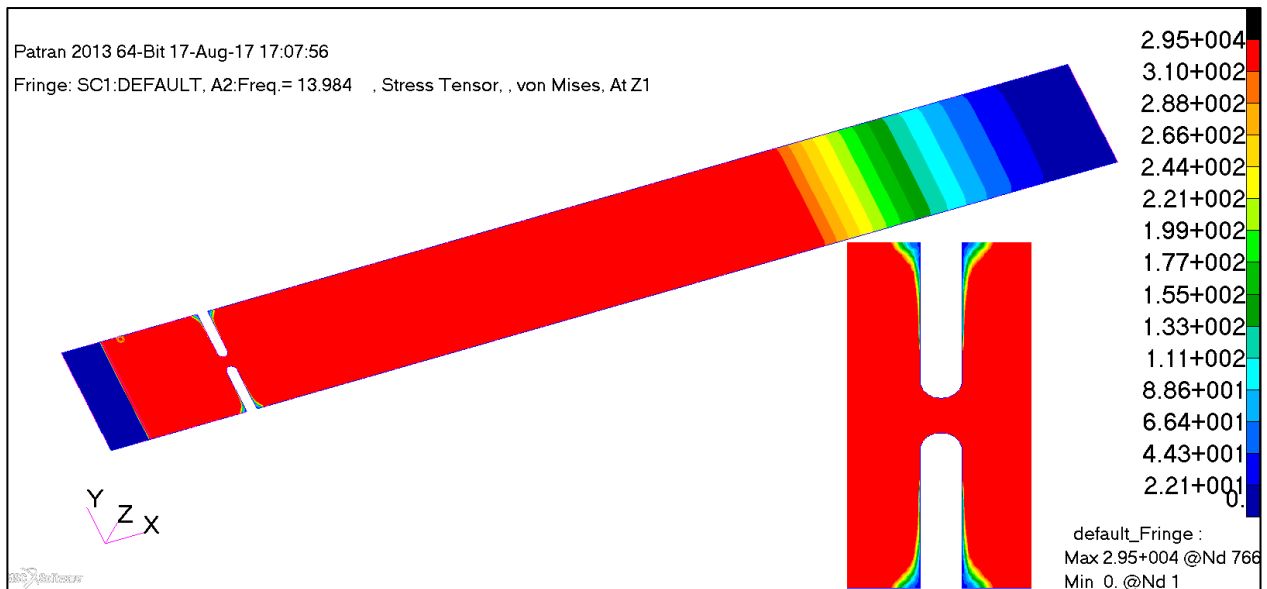


Figure 26: Stress response to unit load at 13.984 Hz, undamped case, [MPa]

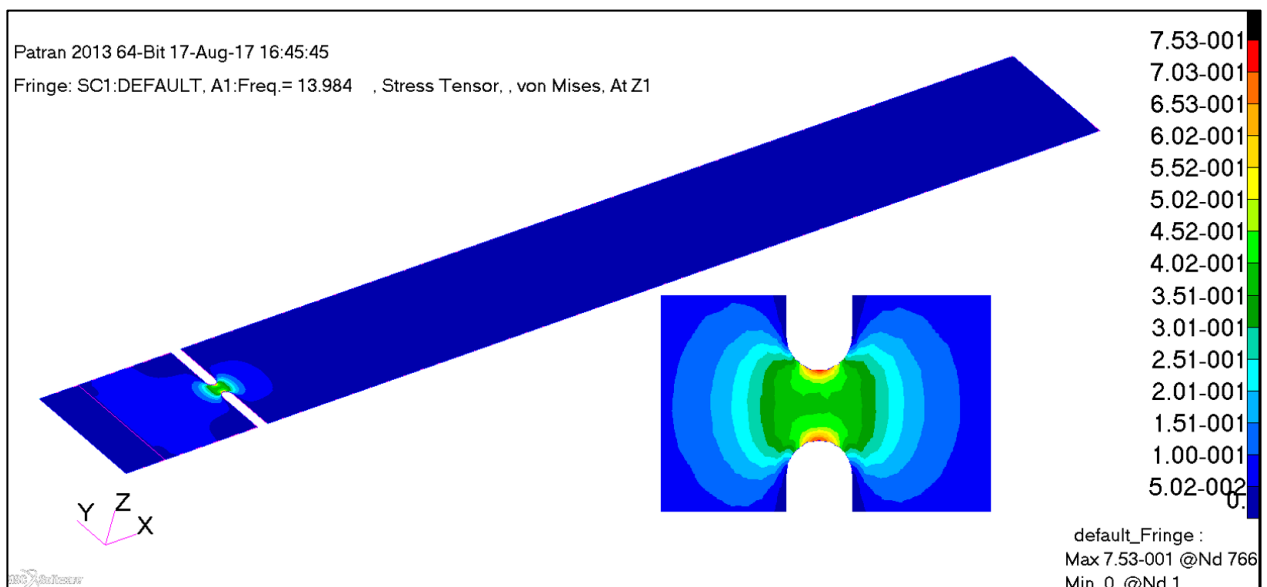


Figure 27: Stress response to unit load at 13.984 Hz, with modal damping case, [MPa]

Due to the Stress-Life method is used for vibration fatigue analysis, the results of the analyses are very sensitive to the stress frequency response profile. The combined stress frequency response plots of the two analyses are given in Figure 28.

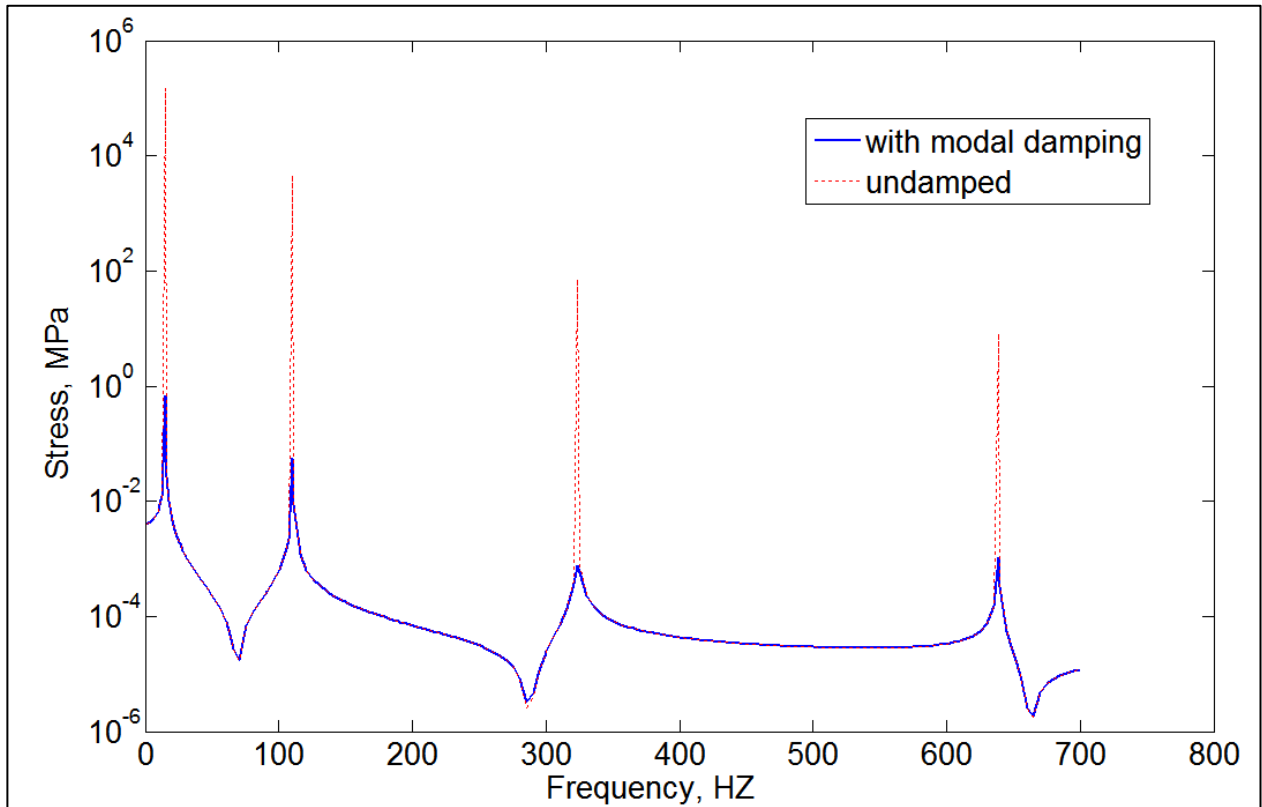


Figure 28: Stress frequency response profiles of the two analyses

Close view of the undamped and damped stress frequency response plots around the first mode is given in Figure 29.

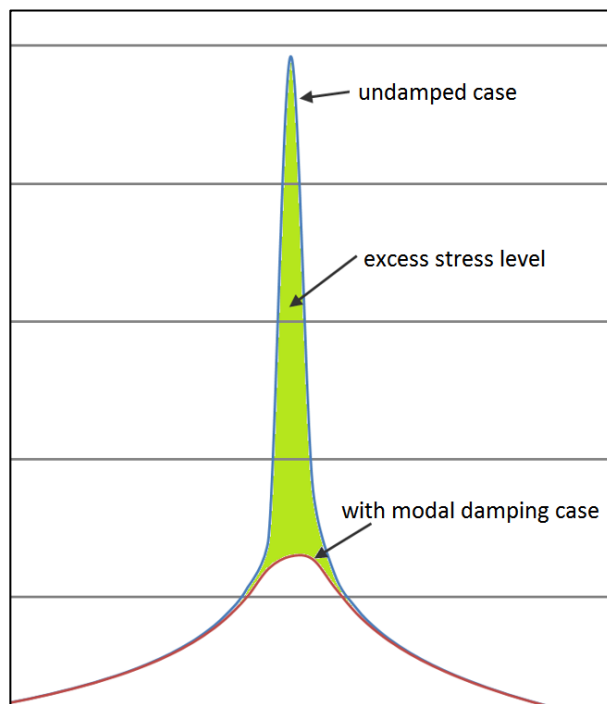


Figure 29: Close view of the undamped and with modal damping cases stress frequency response plots around the first mode

It is concluded that due to the sensitivity of the Stress-Life approach to the stress frequency response profiles, fatigue life results of the notched beam for the undamped and damped cases differ significantly. The excess area, which is highlighted in Figure 29, affects the fatigue life of the notched beam and accounts for the significant difference between the fatigue lives of the notched beams which are obtained by performing undamped and damped vibration fatigue analysis.

CONCLUSION

In this study the effect of including modal damping on the fatigue life results obtained by vibration fatigue analysis is investigated. It is shown that the frequency domain fatigue analysis is very sensitive to the stress frequency response profile of the mechanical systems which is significantly affected by the modal damping. For the notched beam example given in the present study, when modal damping is included in the vibration fatigue analysis, it is seen that the fatigue life of the notched beam increases significantly. In the present study modal damping of the notched beam has been obtained by vibration tests. In general it is recommended to use the modal damping obtained in vibration tests to use in vibration fatigue analysis performed in frequency domain for accurate fatigue life estimations. If the modal damping ratios are not available or the conducting the modal test of the mechanical system is not possible, then one can use the constant damping ratio such as 0.02 for aluminum. However modal damping values depend on the mechanical system configurations, the material conditions used and especially constraint mechanisms. Therefore, without modal test, it is not possible to obtain accurate modal damping ratios, and perform vibration fatigue analysis.

References

- Bhat, S. and Patibandla, R. (2011) *Metal Fatigue and Basic Theoretical Models: A Review, Alloy Steel - Properties and Use*, Dr. Eduardo Valencia Morales (Ed.), InTech, DOI: 10.5772/28911.
- Bishop, N.W.N. (1999) *Vibration fatigue analysis in the finite element environment*, XVI encuentro del grupo español de, fractura, Spain.
- Bishop, N. W. M. and Sherratt, F., *Finite Element Based Fatigue Calculations*, NAFEMS LTD, 1st Edition, November 2000, U.K.
- Dirlik, T., *Application of Computers in Fatigue Analysis*, Ph.D. Thesis submitted to Department of Engineering, University of Warwick, Coventry, UK, January 1985.
- Eldoğan, Y., *Vibration Fatigue Analysis of Structures Installed on Air Platforms*, M.Sc. Thesis submitted to Department of Mechanical Engineering, METU, Ankara, Turkey, Feb 2012.
- Fatemi and Yang, L., *Cumulative Fatigue Damage and Life Prediction Theories: A Survey of the State of the Art for Homogeneous Materials*, Int. J. Fatigue, Vol. 20. No. 1, pp.9-34, 1998.
- Koçer, B., *Vibration Fatigue Analysis of Structures under Broadband Excitation*, M. Sc. Thesis Submitted to Department of Mechanical Engineering, METU, Ankara, Turkey, June 2010.
- Lee, Pan, Hathaway and Barkey, *Fatigue Testing and Analysis (Theory and Practice)*, Elsevier Butterworth-Heinemann, Burlington, MA, USA, 2005.
- MSC. Software, *Dynamic Analysis User's Guide*, MSC Nastran 2013.1 Documentation, Chapter 4-Frequency Response Analysis, November 2013.
- Teixeria, M. G., *Random Vibration Fatigue Analysis of a Notched Aluminum Beam*, International Journal of Mechanical Engineering and Automation, Volume 2, No 10, pp. 425-441, 2015.